

Available online at www.sciencedirect.com**ScienceDirect**

Procedia Structural Integrity 2 (2016) 1295–1302

Structural Integrity

Procediawww.elsevier.com/locate/procedia

21st European Conference on Fracture, ECF21, 20-24 June 2016, Catania, Italy

Numerical analysis of a custom-made pelvic prosthesis

¹G. La Rosa*, ¹C. Clienti, ²S. Di Bella, ¹F. Rizza¹*Department of Industrial Engineering, University of Catania, Viale Andrea Doria, 6 - 95125 Catania, Italy*²*MT Ortho s.r.l., Via Fossa Lupo, 95025 Aci S. Antonio, Catania, Italy*

Abstract

In recent years, 3D-printing technologies are able to fabricate complex shapes of a custom designed component by adding material layer-by-layer from the bottom up on top of each other. Electron Beam Melting (EBM) is a technique capable of manufacturing fully solid metallic parts, using a high-intensity electron beam to melt powder particles in layers in order to form finished components.

Aim of this paper is to perform a FEM analysis of custom-made implant in order to calculate the stress-strain state under daily activities loading. To this purpose, geometry, mechanical properties and boundary conditions have to be known. Geometry was reconstructed with a reverse-engineering process while loading conditions were obtained from literature. Ti6Al4V mechanical properties were determined experimentally with tensile testing. A deeper local analysis was carried out in order to simulate bone-screw interface to define if daily activities can cause bone resorption.

Copyright © 2016 The Authors. Published by Elsevier B.V. This is an open access article under the CC BY-NC-ND license (<http://creativecommons.org/licenses/by-nc-nd/4.0/>).

Peer-review under responsibility of the Scientific Committee of ECF21.

Keywords: Pelvis prostheses; Custom-made prostheses; 3D Electron Beam Melting; FE analysis

1. Introduction

Metal orthopedic joint are fabricated from wrought or cast bar stock by CNC with very high waste of material and, often, significant cost. Moreover, these joints are mass-produced components, which are difficult to realize and sometime inaccurate with patients who need major resection. In these situations, custom-designed implant components are required. In recent years, 3D printing technologies have been developed and can be applied in orthopedics to facilitate the reconstruction of complex shapes bone parts. These rapid prototyping processes allow synthesize metal powder, in particular Ti alloy, and can be used to manufacture components with specific geometric

* Corresponding author. Tel.: +390957382413; fax: +39095337994;
E-mail address: glarosa@dii.unict.it

parameters, such as relative distance from internal organs and biological system, assuring the biomechanics of musculoskeletal system (Harrysson, and Cormier (2005), Harrysson et al. (2008), Thundal (2008), Al-Bermani et al. (2010), Marin et al. (2013), Peng-Cheng et al. (2014)).

Whereas on one hand skull cup reconstruction does not require any specific strength conditions, on the other hand bone substitutions, as part of locomotor system, must assure cinematic and dynamic functionality in order to preserve high motion range. In particular, referring to hip joint, the movements that can be carried out at this joint are flexion, extension, abduction, adduction and medial/lateral rotation. The direction and the amount of this movements depends on the activities the person is able to perform, ranging from monopodal stance to more strenuous activities like going upstairs and stumbling.

Within the collaboration between University of Catania and MT Ortho, a company specialized in prosthesis designing and manufacturing, a custom made pelvic implant was developed and inserted in a patient who underwent a reconstructive hemipelvectomy. The prosthesis was created using EBM process, an additive manufacturing techniques mainly used for metallic biomaterials to build physical components from digital CAD models by building the part layer by layer.

Aim of this paper is the study of the stress-strain state in a custom-made pelvis caused by daily activities, using FE analysis. Due to its complex shape, a reverse engineering process was performed to acquire the real dimensions of the implant (Fig. 1). Beside geometry, in order to carry out FE analysis, mechanical characteristics of the Ti alloy were defined by experimental tests and boundary conditions were applied from literature (Pauwels (1979), Sutton et al. (2009)). In particular, the main source of acting loads in the musculoskeletal system for orthopedic biomechanics is the telemetric in vivo measurement (Sutton et al. (2009)), while the proprieties of EBM Titanium material were determined experimentally using Digital Image Correlation (D.I.C.) and thermographic analysis.

A second and deeper numerical analysis was carried out to the simulate bone–screw interface zones, in order to define if daily activities can cause local bone resorption. The reaction forces, obtained from the previous analysis, were used as loading condition while material and geometry were already known.

2. Experimental investigation

Mechanical characterization was carried out performing tensile tests using a *Z-100 Zwick Roell* testing machine (100 kN maximum load) and with a displacement rate of 2 mm/min.

The tensile specimens have flat dog-bone shape with a gauge length of 25 mm and a 6x3.5 mm² cross-section. Different tensile specimens were fabricated using EBM process with different growing directions, in order to investigate the influence of orientation (A, B) on the mechanical characteristics as show in Fig. 2.

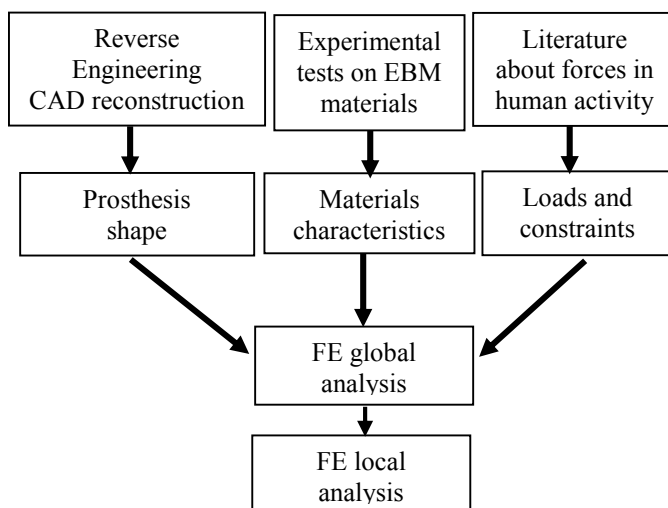


Fig. 1. Flow diagram.

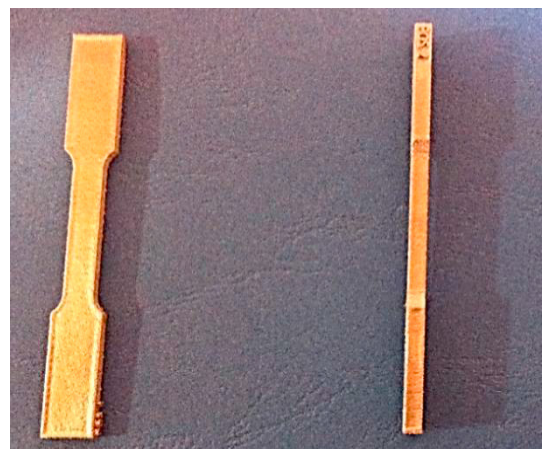


Fig. 2. Specimen orientation: A left; B right.

2.1. Digital Image Correlation: experimental setup and procedure

D.I.C. methodology was preferred as non-contact optical technique to measure strain instead of strain gauges techniques. The D.I.C. method compares digital images for various small regions (subsets) throughout the images before and after deformation, locating the position of each subsets after deformation through digital image analysis. For this study, 2D D.I.C. was used and the standard measurement layout was reported in Fig.3 (a). The flat specimens were mounted in the tensile machine and the optical axis of the camera was perpendicular with respect to the measurement surface. During tensile tests, PixeLink PI-B958F camera, with a resolution of 1600x1200 pixels at 7.5 fps, was used to acquire the images that were analyzed with *Digital Image Correlation and Tracking algorithm*.

Before starting the test, the specimen needs to be prepared by the application of a random dot pattern to its surface. The speckle pattern can be applied by painting the surface with a thin layer of white paint and, then, applying a black paint to create the black speckles as show in Fig.3 (b).

A subset size of 10x10 pixels was chosen for this study, corresponding to a subset of about $75 \times 75 \mu\text{m}^2$.

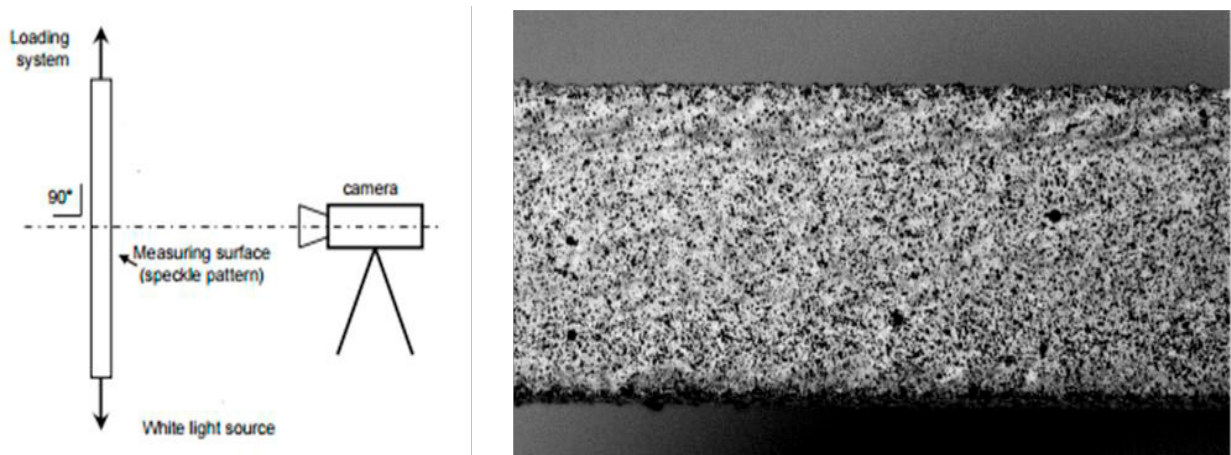


Fig. 3. (a) D.I.C. layout; (b) Speckle pattern used for D.I.C.

2.2. Thermographic analysis: experimental setup and procedure

During tensile testing, a thermographic analysis was simultaneously performed. The surfaces emitting various amounts of infrared radiation can be differentiated on the thermogram by various colors or brightness levels as different isothermal areas. According to thermoelastic theory, during tensile test the temperature of the material decreases linearly. It has been proven that when the deviation from the linearity starts the plastic process begun, limiting the decrease and initiating the production of plastic heat. This level can be correlated to the total elastic behavior of the material and, consequently, with the endurance limit. When the curve invert the training (corresponding to the minimum), the macroscopic plastic phenomena predominate on the thermoelastic effect. Correlating this phase with the current load, yield stress can be determined in accurate way.

The ThermaCAM SC3000 infrared camera, with a resolution of 320x240 pixels at 8 fps, has been used to acquire thermograms. It was positioned at a distance of 0.5 m from the sample surface, as show in Fig. 4 (a). Before testing, the specimen was covered with black paint to make the radiation rate on the surface uniform and to avoid the reflection and maximize the emissivity.

ThermaCAM Researcher software was used to process images and, then, to measure the temperatures at selected spots. For this study, three spots were used in upper, medial and lower position, as show in Fig. 4 (b) to acquire directly the behavior of the thermal variations in different areas and to verify the uniformity of the stress on the detected area.

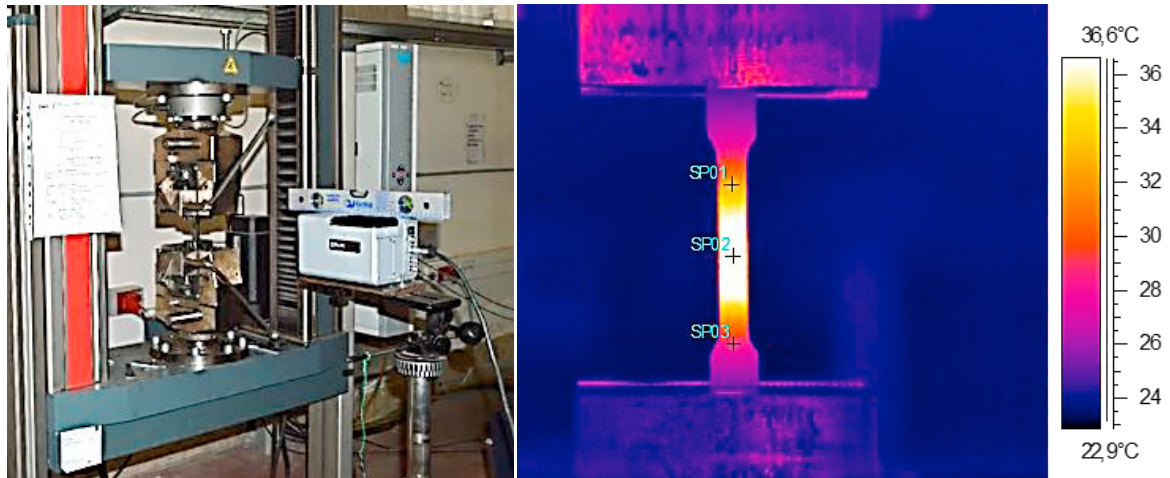


Fig. 4- (a) Layout for thermographic analysis; (b) Spot selected to detect temperature by ThermoCAM Researcher software.

3. Analysis of results

3.1. Digital Image Correlation results

After processing every image with *Digital Image Correlation and Tracking Algorithm* using Matlab, strain can be determined for each specimen. As shown in Fig. 5, the first 10 s show to a very slow linear increase, corresponding to linear elastic behavior of the material. After that, strain increases faster and rapidly until specimen brakes.

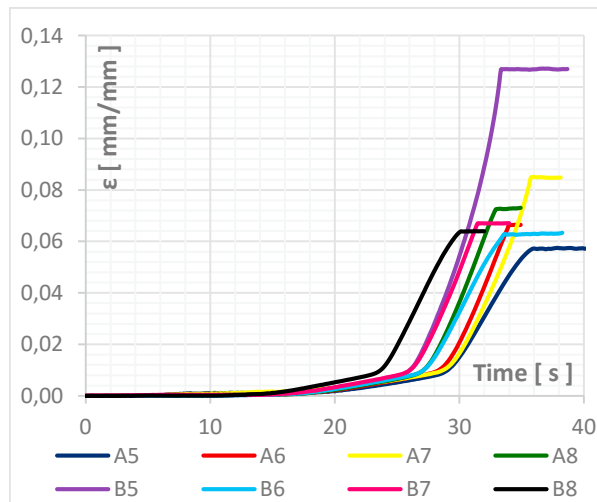


Fig.5 – Strain during time for each specimen.

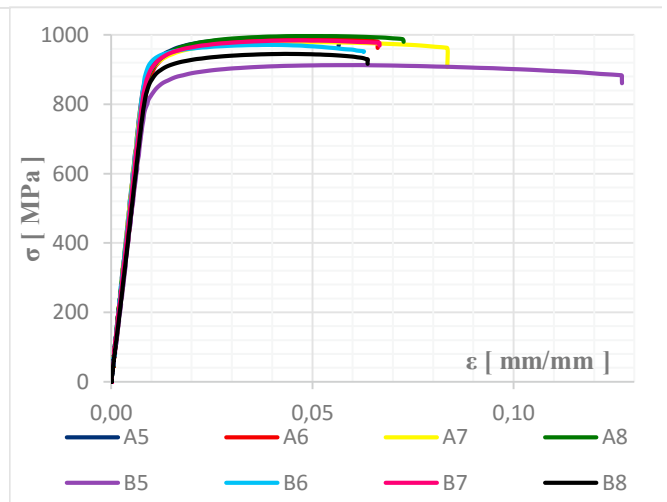


Fig.6 – σ - ϵ curve for Ti6Al4V.

Correlating strain with stress, acquired from testing machine, stress-strain curve can be obtained as displayed in Fig.6. It is possible to distinguish a similar behaviour for all the specimen analysed so the influence of orientation is negligible. These results confirm that Ti6Al4V produced by EBM process has an almost linear elastic isotropic behaviour. Average Young's modulus and yield strength are, then, 105 GPa and 880 MPa, respectively, in good agreement with those found in literature. These values will be used later as material characteristics during FE analysis.

3.2. Thermographic analysis results

Processing and plotting thermographic data at various spots, a temperature decrease can be noted. During the first seconds the temperature difference is nearly zero therefore, according to D.I.C., strain is negligible, corresponding to the toe region of the load. After this initial region, temperature starts decreasing linearly with low slope as displayed in Fig.7. Green line expresses thermoelastic effect with two different phases: totally elastic and macroscopically elastic, the latter deviating from the linearly just when the local plastic process begun. At the end of this phase, when the trend of the temperature increases, the plastic phenomenon become macroscopic and the yield point is reached (Clienti et al. (2010), Risitano et al. (2011, 2013, 2015), La Rosa and Risitano (2014)).

Correlating this phase with the current load, yield stress can be determined in accurate way. Yield strength obtained by the standard procedure and that calculated by thermography show error lower that 5%, so it is possible to assume that thermographic method can be validated as another technique to calculated yield strength.

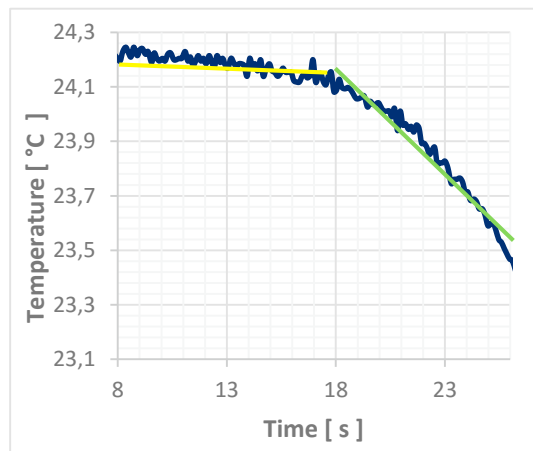


Fig.7. Temperature vs. time of SP01 in the first.

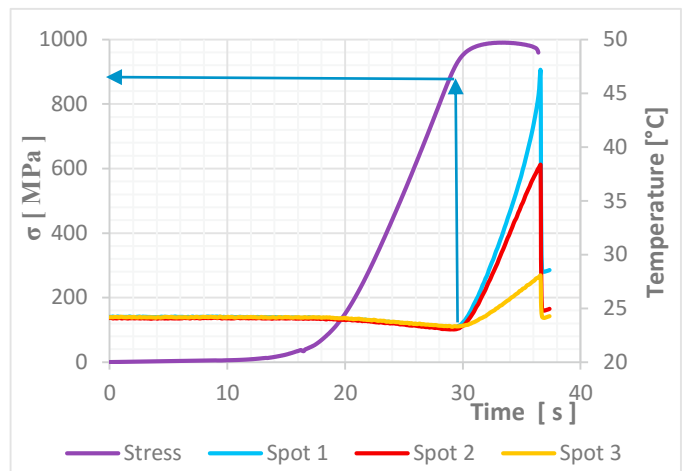


Fig.8. Temperature vs. time and yield point determination.

4. FEM Analysis

Finite Element Analysis (FEA) of the prosthesis was carried out in order to calculate stress and strain for daily activities. The original implant data were given as point cloud data in STL format and converted, using reverse engineering, into a solid CAD model using ANSYS Spaceclaim. The error between the real implant and the one recreated with reverse engineering was 0.37%. The 3D CAD model was imported into the ANSYS Workbench software to prepare the FEA. Loads, boundary conditions and material models were defined. The mesh process was performed using fine mesh and the model has 103.499 nodes e 59.408 elements.

Ti6Al4V mechanical proprieties were determined experimentally while both cortical and cancellous bone mechanical proprieties were researched in literature (Evans (1973), Katz and Meunier (1987), Rho et al. (1998), Cowin and Doty (2007)). Particularly, Young's modulus was considered 17 GPa and 2.2 GPa for cortical bone and cancellous bone, respectively.

Three different load conditions, summarized in Table 5 (Johnston and Smidt (1970), Bergmann et al. (2010)), were analyzed and applied to acetabular as show in Fig. 9. The implant was constrained with fixed support on the surface where screws bolt the prosthesis to the bone.

Table 5. Load for different load condition.

Activity	F [N]	F _x [N]	F _y [N]	F _z [N]
Walking	3900	873	540	3761
Going up the stairs	4200	985	1025	3951
Stumbling	11000	2462	1523	10607

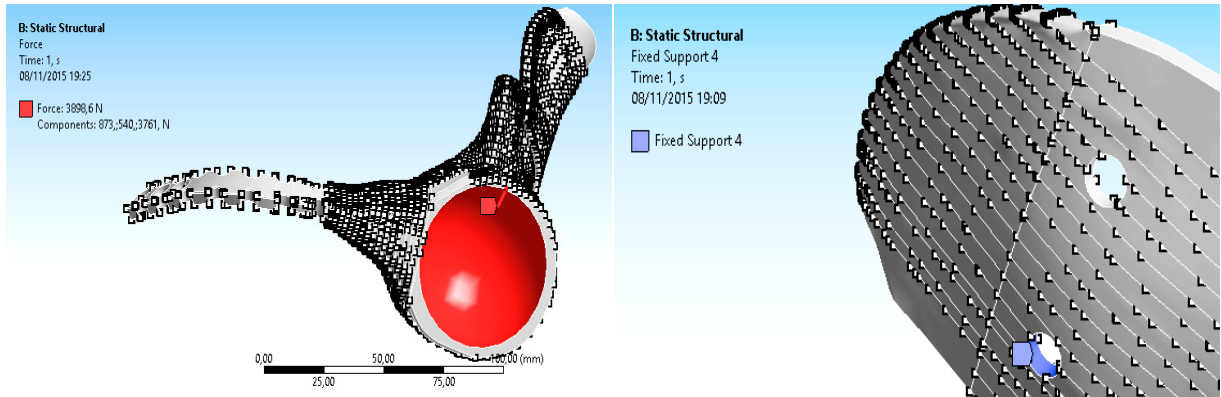


Fig. 9. (a) Load applied on acetabular cup (b); Selection of the constrained surface

Von Mises stress, elastic strain and force reaction were determined for the different loading conditions. In particular, the highest stresses are 258 MPa for walking, di 274 MPa for going up the stairs and 730 MPa for stumbling (Fig. 10). All values are beneath yield stress value.

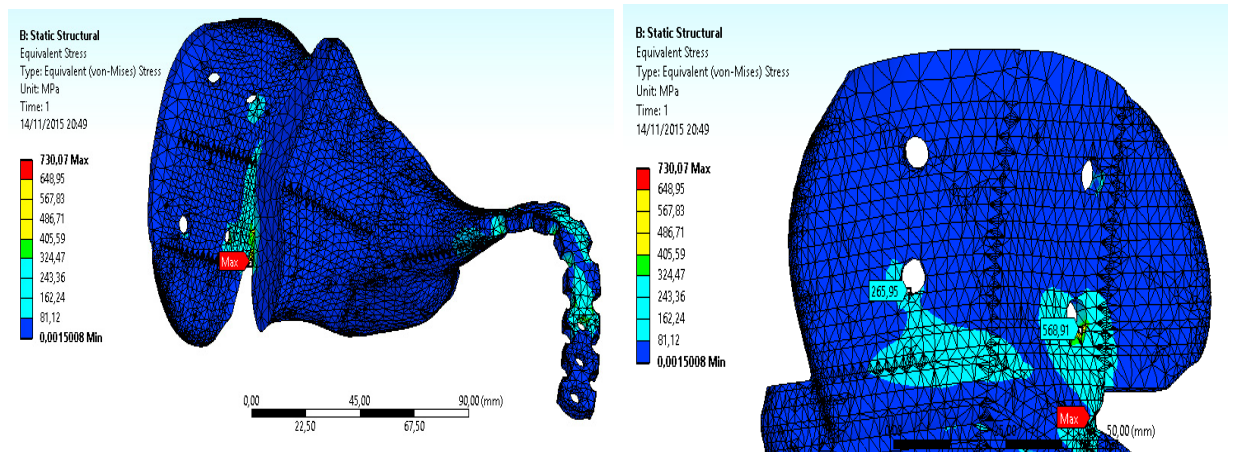


Fig. 10. Elastic stress in different location for stumbling.

The force reactions were used as load condition for bone–screw interface. According to Frost Mechanostat Theory, in order to have physiological state strain must be between 200 and 2500 μ strain (Frost (1994)).

As show in Fig. 11, the prosthesis is attached to the pelvis with different kind of connection: while screws 1–4 use bolt connection with a plate on the other part of the ileum, screw 5–7 are directly connected to the pubic bone. The highest force reaction where calculated for screw 2 and 4 for bolted connection and screw 5 and 6 for direct connection.

In order to simplify the analysis a section of the complete assemble was considered as show in Fig. 11 (b). Cancellous and cortical bone, with different mechanical properties, were identified. The thickness of each layer was obtained with reverse engineer process from the STL file of the real bone.

The analysis was carried out considering only daily activities as walking and going up the stairs using for both model a fine mesh. A frictional coefficient of 0.2 was use to simulate screw–bone contact.

Analizing the result for screw 2 and 4 the strain was ranging from 1200 μ ϵ and 1400 μ ϵ for both activities (Fig. 12). In fact, the highest force reactions correspond to a through bolts connections. Focusing on screw 5 and 6 the strain was between 1500 μ ϵ and 1800 μ ϵ . So, for all configuration strain was in the adaptation range.

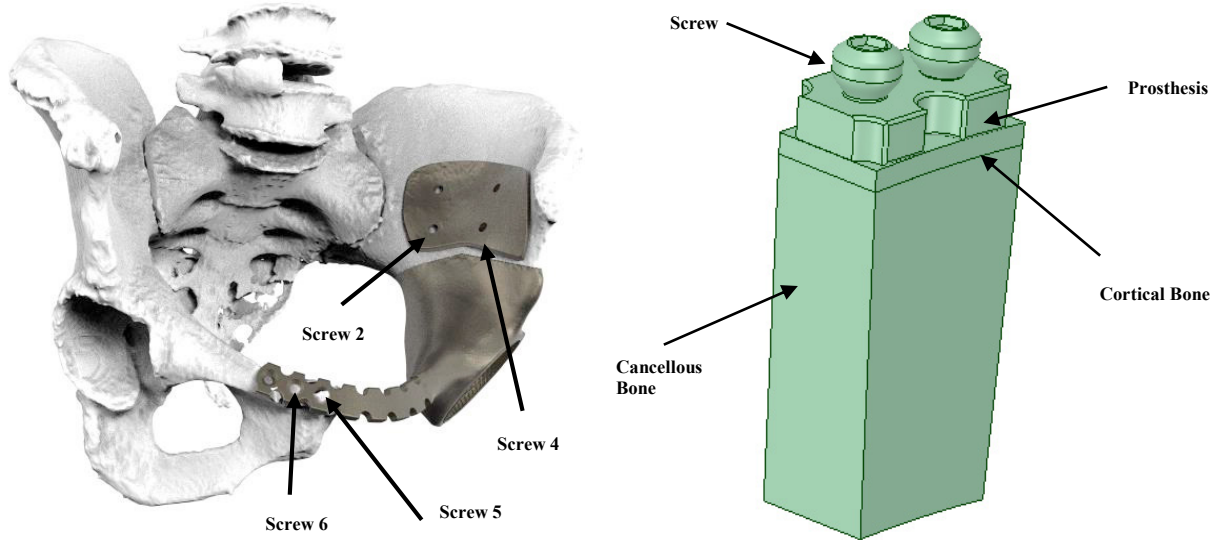


Fig. 11. (a) Different connection for the prosthesis (b) Simplified geometry analyzed in the FEA

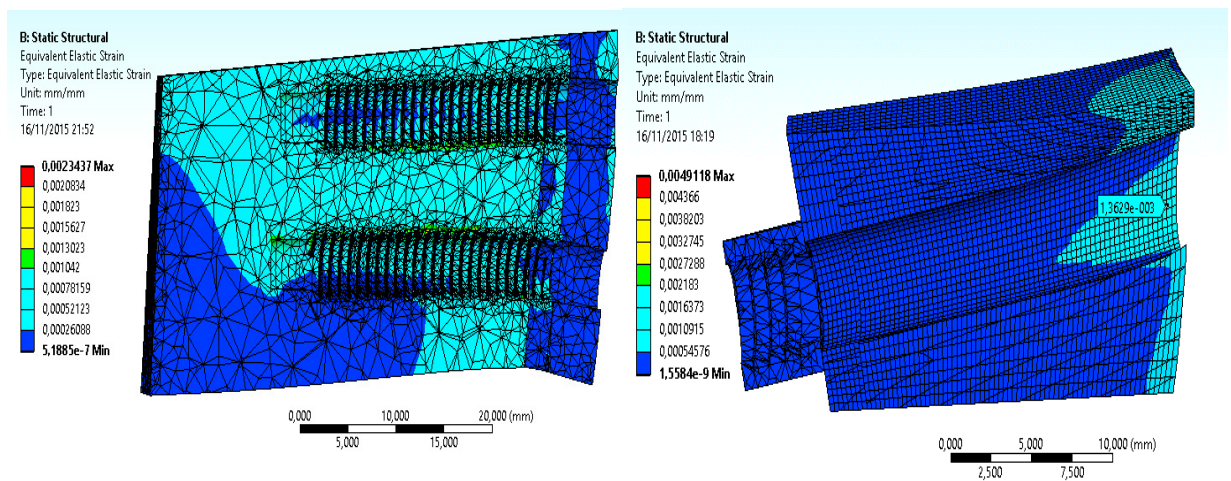


Fig. 12. Strain calculated for screw – bone interface

5. Conclusions

A whole procedure to design a pelvic prosthesis in Ti alloy, produced using the EBM technology by MT Ortho, was performed, involving experimental and simulation activities. Reverse engineering was used to acquire the geometrical information, experimental tests were carried out to define the mechanical properties of the EBM material and data from literature were collected to determinate the loading conditions on the prosthesis.

In particular, in order to define the mechanical characteristics of the material obtained by the EBM process, as this produces the biomechanical element layer-by-layer, different specimens were realized with different growing direction. Finite element analysis, in fact, needs to characterize the material along different direction, due to the morphological complexity of the prosthesis.

Together with the traditional tensile testing, the Digital Image Correlation methodology was used to measure the strain on the specimens, avoiding all the clearances and the deformation of the measuring chain. Moreover, the yield point was defined, as well as with the traditional techniques, also by means of thermographic investigation, able to

highlight the yield point as the minimum of the curve temperature-strain of the sample. The results showed as the growing direction was quite irrelevant on the mechanical characteristics, allowing to consider the material obtained by EBM process as isotropic and homogeneous.

The implant data were given as point cloud data and converted, using reverse engineering, into a solid CAD model with a very low error. The data on the material and the geometry, together with those acquired by literature on the loads produced on the pelvis by the most common (walking) or heavy (going up the stairs or stumbling) human activities, were used to simulate the stress and strain state by a detailed finite element model. All the simulations did not produce dangerous conditions in terms of stress or strain that could indicate overload or bone resorption.

Particular attention was dedicated to the bone-implant interface and to the analysis of the junction regions by screws. A simplified but effective model was considered for connecting the prosthesis to cortical and cancellous bone.

Finally, the used methodology, performed to design a pelvis implant, can be considered an integrated experimental and numerical analysis for custom made prostheses realized by EBM process and assure a better reliability for a success of the biomechanical implant.

References

- Al-Bermani, S.S., Blackmore, M.L., Zhang, W., Todd, I., 2010. The origin of microstructural diversity texture and mechanical properties in electron beam melted Ti6Al4V. *Metallurgical and Materials Transactions A-physical Metallurgy and Materials Science.*, 41, 3422-3434.
- ASTM Standards. F1472-14-Standard Specification for Wrought Titanium-6 Aluminum-4 Vanadium Alloy for Surgical Implant Applications. 2014.
- ASTM Standards F1108-14- Standard Specification for Titanium-6 Aluminum-4 Vanadium Alloy Castings for Surgical Implants. 2014.
- Bergmann, G., Graichen, F., Rohlmann, A., Bender, A., Heinlein, B., Duda, G., Heller, M.O., Morlock, M.M., 2010. Realistic loads for testing hip implants. *Bio-Medical Materials and Engineering*. 210, Vol. 20, 2, 65-75.
- Clienti, C., Fargione, G., La Rosa, G., Risitano, A., Risitano, G., 2010. A first approach to the analysis of fatigue parameters by thermal variations in static tests on plastics. *Engineering Fracture Mechanics*, 77 (11), 2158-2167.
- Evans, F.G., 1973. *Mechanical Properties of Bone*. Springfield, IL : Charles C. Thomas,.
- Cowin, S. C., Doty, S. B., 2007. *Tissue mechanics*. New York, Springer,.
- Frost, H.M., 1994. Wolff's Law and bone's structural adaptations to mechanical usage: an overview for clinicians. *The Angle Orthodontist.*, 64, 3, 174-188.
- Harrysson, O.L.A., Cormier, D.R., 2005. Direct Fabrication of Custom Orthopedic Implants Using Electron Beam Melting Technology. *John Wiley & Sons, Ltd*, 191–206
- Harrysson, O.L.A., Cansizoglu, O., Marcellin-Little, D.J., Cormier, D.R., West, H.A. II, 2008. Direct metal fabrication of titanium implants with tailored materials and mechanical properties using electron beam melting technology. *Mat Sci Eng C*, 28(3), 366–373.
- Johnston, R.C., Smidt, G.L., 1970. Hip motion measurements for selected activities of daily living. *Clinical Orthopaedics and Related Research.*, 72, 205-15.
- Katz, J.L., Meunier, A. , 1987. The elastic anisotropy of bone. *Journal of Biomechanics*. 20, 11 – 12, 1063–1070.
- La Rosa, G., Risitano, A., 2014. Evaluation of the fatigue limit of materials in static test using thermal analysis: Effect of the cross-head speed. *Key Engineering Materials*, 577-578, 69-72.
- Marin, E., Pressacco, M., Lanzutti, A., Turchet, S. , Fedrizzi L., 2013. Characterization of grade 2 commercially pure trabecular Titanium structures. *Materials Science and Engineering C*, 2648–2656.
- Pauwels, F., 1979. *Biomechanics of the Locomotor Apparatus: Contributions on the Functional Anatomy of the Locomotor Apparatus*. New York, Springer.
- Peng-Cheng, L., Yun-Ji Y., Run L., He-Xi S., Jin-Peng, G., Yong, Y. , Qi, S. , Xing, W., Ming, C., 2014. A study on the mechanical characteristics of the EBM-printed Ti-6Al-4V LCP plates in vitro. *Journal of Orthopaedic Surgery and Research*. 9, 106.
- Rho, J.Y., Kuhn-Spearing, L., Zioupos, P., 1998. Mechanical properties and the hierarchical structure of bone. *Medical Engineering & Physics.*, 20, 92-102.
- Risitano, A., Clienti, C., Risitano, G., 2011. Determination of fatigue limit by mono-axial tensile specimens using thermal analysis. *Key Engineering Materials*, 452-453, 361-364.
- Risitano, A., Risitano, G., 2013. Determining fatigue limits with thermal analysis of static traction tests. *Fatigue and Fracture of Engineering Materials and Structures*, 36, 7, 631-639.
- Risitano, A., La Rosa, G., Geraci, A., Guglielmino, E., 2015. The choice of thermal analysis to evaluate the monoaxial fatigue strength on materials and mechanical components. *Proceedings of the Institution of Mechanical Engineers, Part C: Journal of Mechanical Engineering Science*, 229, 7, 1315-1326.
- Sutton, M.A., Orteu, J.J., Schreier, H., 2009. *Image Correlation for Shape, Motion and Deformation Measurements: Basic Concepts, Theory and Applications*. Springer.
- Thundal, S., 2008. Rapid manufacturing of orthopaedic implants. *Advanced Materials & Processes*, 166 , 60–62.